ESTIMATION OF THE CARDIAC EJECTION FRACTION FROM IMAGE STATISTICS

Mariam. Afshin[⋆⋆]*, Ismail. Ben Ayed*[†]*, Ali. Islam*[|]*, Aashish. Goela*[‡]*, Ian. Ross*[‡]*, Terry. Peters*[⋆⋆]*, Shuo. Li*[†]

[⋆] University of Western Ontario,[*]Robarts Research Institute, [†]GE Healthcare,
[|]St. Joseph's Health Care [‡]London Health Science Center {London, Ontario, Canada}

ABSTRACT

The Cardiac Ejection Fraction (EF) is an essential criterion in cardiovascular disease prognosis. In clinical routine, EF is often computed from manually or automatically segmenting the Left Ventricle (LV) in End-dyastole and End-systole frames, which is prohibitively time consuming and needs user interactions. In this paper, we propose a method to minimize user effort and estimate the EF directly from image statistics via machine-learning techniques, without the need for comprehensive segmentations of all the MRI images in a subject dataset.

From a user-provided segmentation of a single image, we build a statistic based on the Bhattacharyya coefficient of similarity between image distributions for each of the images in a subject dataset (200 images). We demonstrate that these statistical features are non-linearly related to the LV cavity areas and therefore can be used to estimate the EF. We used Principal Component Analysis (PCA) to reduce the dimensionality of the features and areas. Then, an Artificial Neural Network (ANN) was used to predict the LV cavity areas from the dimension-reduced features. The EF is finally estimated from the obtained areas.

1. INTRODUCTION

The ejection fraction (EF) is an important indicator of long-term prognosis for patient with coronary artery disease. As the left ventricle (LV) is the heart's main pumping chamber, the EF is usually measured using information from the LV [1–3]. The EF may decrease in the case of a heart attack or other problems related to the heart valves or muscle and is therefore one of the most important criteria for diagnosing cardiovascular diseases.

In routine clinical use, the EF is often computed from several images in a cardiac sequence using manual segmentation, which is prohibitively time consuming. Automatic LV segmentation can be used to compute the EF, but is still acknowledged as a challenging, computationally expensive task, which has attracted impressive research attention in recent years. Existing LV segmentation algorithms are based on traditional techniques, such as thresholding, region-growing, edge detection and clustering [4–6], and energy minimization techniques such as graph cuts [7,8], active contours/level sets [9, 10], as well as active appearance and shape models [11]. In general, segmentation algorithms require a careful user initialization, intensive training, and are computationally expensive. Furthermore, the ensuing segmentation results depend significantly on the choice of a set of *ad hoc* parameters and training data, which may yield high errors in the computation of the EF. These difficulties inherent to segmentation algorithms impede the automatic estimation of the EF in routine clinical use. A recent comprehensive review of cardiac image segmentation and its challenges can be found in [12].

We believe that there are other characteristics of the images that can be computed with less effort, but that nevertheless correlate strongly with the EF. One such technique that we describe below is based on machine learning, from image statistics, removing the need for image segmentation. From a simple user input in one single image, we build for all the images in a subject dataset (200 images) a statistic based on the Bhattacharyya coefficient [13] of similarity between image distributions. We demonstrate that these statistics are non-linearly related to the LV cavity areas (cf. Fig. 2) and therefore can be used to estimate the EF directly via an Artificial Neural Network (ANN).

The proposed method consists of four main steps: (1) Image acquisition, (2) Building Image Statistics, (3) Applying the Artificial Neural Network, and (4) Estimating Ejection Fraction. The preliminary results over 6 subjects demonstrate that the estimated EFs correlated very well with those obtained from manual segmentations.

2. ESTIMATING LEFT VENTRICLE VOLUMES FROM IMAGE STATISTICS

2.1. Building image statistics

Let $\mathscr{I}$ be a Cardiac MRI sequence containing I frames[1], each comprising J slices[2]: $\mathscr{I}_{i,j}$: $\Omega \subset \Re^2 \rightarrow \Re^+$ with $(i,j) \in [1 \ldots I] \times [1 \ldots J]$. To introduce how we build an image statistic related to the LV cavity area for each image $\mathscr{I}_{i,j}$, $(i,j) \in [1 \ldots I] \times [1 \ldots J]$, let us consider the following defi-

[1]The number of frames I is typically equal to 20 or 25.
[2]The number of slices J is typically equal to 10.

nitions. Let $\mathbf{I}$ be a reference image[3] whose segmentation is assumed given, and $\Gamma_{in}, \Gamma_{out} : [0,1] \rightarrow \Omega$ respectively denote the corresponding manual endo and epicardium boundaries, as depicted in the typical example in Fig.1 (a). Let us now superimpose the manually defined epicardial boundary, Γ_{out}, to the rest of the images in the dataset, as shown in Fig.1 (b) and Fig.1 (c), and compute the corresponding image statistics.

To this end, let $\mathbf{R}_\Gamma \subset \Omega$ be the region enclosed within Γ, $\Gamma \in \{\Gamma_{in}, \Gamma_{out}\}$, and $P_{\mathbf{R}_\Gamma, I}$ the kernel density estimate of the distribution of an image $I \in \mathscr{I}_{i,j}$, $(i,j) \in [1 \ldots I] \times [1 \ldots J]$, within region $\mathbf{R}_\Gamma$:

$$P_{\mathbf{R}_\Gamma, \mathscr{I}}(z) = \frac{\int_{\mathbf{R}_\Gamma} K(z - \mathscr{I}) dx}{\int_{\mathbf{R}_\Gamma} dx} \quad (1)$$

with K the Gaussian kernel [13]. Now consider the following measure of similarity between the intensity distribution inside the region corresponding to the LV cavity in the reference image ($P_{\mathbf{R}_{\Gamma_{in}}, \mathbf{I}}$) and the distribution of the whole left ventricle, i.e., the region within the epicardium boundary Γ_{out} (refer to the red curve in the first row in Fig.1.), in each image $\mathscr{I}_{i,j}$, $(i,j) \in [1 \ldots I] \times [1 \ldots J]$:

$$\beta^{i,j} = \mathbf{B}(P_{\mathbf{R}_{\Gamma_{in}}, \mathbf{I}}, P_{\mathbf{R}_{\Gamma_{out}}, \mathscr{I}_{i,j}}), \quad (2)$$

where $\mathbf{B}(f,g)$ is the Bhattacharyya coefficient measuring the amount of overlap (similarity) between two distributions f and g:

$$\mathbf{B}(f,g) = \int_{R^+} \sqrt{fg} dz \quad (3)$$

We expect that measure $\beta^{i,j}$ is related to the cavity area in image $\mathscr{I}_{i,j}$. This is demonstrated experimentally by the typical example in Fig.1 and the corresponding similarities between the variations of the Bhattacharyya statistics, $\beta^{i,j}$, and cavity areas in Fig.2. Such similarities make sense because the more overlap between the distributions of the cavity and the LV, the higher the cavity area.

2.2. Artificial Neural Network (ANN) estimation of LV cavity areas

We estimate the nonlinear relation between the cavity areas and the Bhattacharyya statistics we built by training via a back propagation Artificial Neural Network (ANN), a powerful machine learning technique [14].

We constructed an Artificial Neural Network (ANN) to determine the nonlinear relation between the Bhattacharyya statistics and the corresponding LV cavity areas (refer to Fig.2 for an illustration of such non-linear relation). Following a back propagation ANN, our feed-forward network consists of five layers, three hidden, one input, and one output.

[3]For each subject, the reference image is chosen to be an end-diastolic, mid-cavity slice.

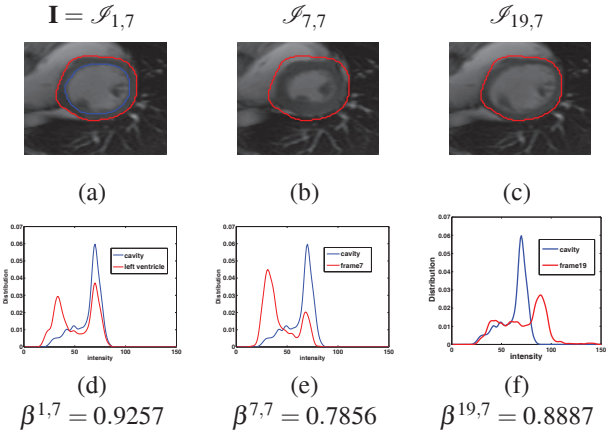


Fig. 1. Computing image statistics from a given delineation of a single reference image: (a) reference image (red curve: Γ_{out}, blue curve: Γ_{in}); (b) and (c) subsequent images; (d), (e), and (f) corresponding distributions and Bhattacharyya measures of overlap ($\beta^{i,j}$). *We observe that the variations of $\beta^{i,j}$ are similar to the variations of the LV cavity areas*

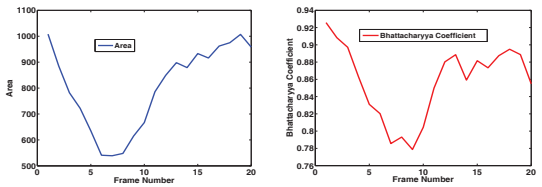


Fig. 2. (a) A typical example which shows the variations of LV cavity areas obtained from manual segmentations; (b) A typical example which shows the variations of the Bhattacharyya image statistics.

Let $P_{1,200}$ be a single row matrix containing the Bhattacharyya statistics, and $T_{1,200}$ be a single row matrix containing the LV cavity areas:

$$P_{1,200} = [P^1, ..., P^j, ..., P^{10}];\ T_{1,200} = [T^1, ..., T^j, ..., T^{10}], \quad (4)$$

st.

$$P^j = \left[\beta^{1,j} \ldots \beta^{i,j} \ldots \beta^{20,j}\right],\ T^j = \left[a^{1,j} \ldots a^{i,j} \ldots a^{20,j}\right]. \quad (5)$$

Thus, for each subject, the Bhattacharya statistics, $P_{1,200}$, and the corresponding LV cavity areas, $T_{1,200}$, can be considered as a point in 200-dimensional space and can be projected to a lower dimentional space. To reduce the dimensionality of the inputs and outputs, we used principal component analysis (**PCA**) to transform 200 possibly correlated variables into a smaller set of uncorrelated variables (the first five components in our case):

$$IN_{1,5} = \mathbf{PCACOV}(P_{1,200}); \quad OUT_{1,5} = \mathbf{PCACOV}(T_{1,200}), \tag{6}$$

where **PCACOV** is the **PCA** transform function and $IN_{1,5}$ and $OUT_{1,5}$ denote the transferred inputs and outputs respectively.

2.2.1. Training:

The next step is to train the network using the transferred inputs ($IN_{1,5}$) and outputs ($OUT_{1,5}$). The network we built estimates the following non-linear mapping:

$$OUT_{1,5} = \mathbf{F}(IN_{1,5}), \tag{7}$$

where **F** is a nonlinear transfer function of three layers, one input containing two neurons and one output containing one neuron, both based on the linear function, as well as one hidden containing five neurons and based on the hyperbolic tangent function, a common choice in the neural network literature [14].

$$INPUT_{5,19} = [(IN^1)^{-1}, ..., (IN^a)^{-1}, ..., (IN^{19})^{-1}] \tag{8}$$

$$st. \quad {IN^a}_{1,5} = \mathbf{PCACOV}(P_{1,200})$$

$$OUTPUT_{5,19} = [(OUT^1)^{-1}, ..., (OUT^a)^{-1}, ..., (OUT^{19})^{-1}] \tag{9}$$

$$st. \quad OUT^a_{1,5} = \mathbf{PCACOV}(T_{1,200})$$

2.2.2. Testing:

To validate this procedure, *we employ a leave-one-out approach, where the test subject dataset was excluded from the training data*. For the current testing subject dataset, the LV cavity areas were estimated using the transferred subject Bhattacharyya statistics and the learned non-linear mapping **F** followed by applying inverse PCA ($\mathbf{PCACOV}^{-1}$).

$$OUT_{test\,1,5} = \mathbf{F}(IN_{test\,1,5}); \; T_{test\,1,200} = \mathbf{PCACOV}^{-1}(OUT_{test\,1,5}) \tag{10}$$

2.3. Estimating the cardiac ejection fraction from image statistics

Let V_{ES} and V_{ED} denote the smallest (end-systolic) and largest (end-diastolic) volumes of the LV in a cardiac cycle, respectively. The cardiac ejection fraction, EF, is given by:

$$EF = \frac{V_{ED} - V_{ES}}{V_{ED}}, \tag{11}$$

where numerator measures the blood volume pumped by the left ventricle. We computed V_{ES} and V_{ED} by integrating the computed LV cavity areas in the sagittal direction.

EF_M	EF_A
0.5555	0.5234
0.5973	0.5437
0.4889	0.5148
0.642	0.6623
0.4832	0.464
0.5109	0.5119

Table 1. Statistical measures of the conformity between automatically and manually computed EFs and computation time (in seconds)

3. EXPERIMENTAL EVALUATIONS AND COMPARISONS

A set of 2D short-axis cine magnetic resonance (MR) images of 20 subjects was acquired through the cardiac cycle on a 1.5T scanner with fast-imaging employing steady-state acquisition (FIESTA) image sequence mode. The acquisition parameters were as follows: TR=2.98 ms, TE=1.2 ms, flip angle=30 degree, and slice thickness=10 mm. Each subject's dataset consists of 20 frames, each comprising 10 slices.

We used the proposed method to automatically compute the LV cavity areas on each slice, thereby estimating the LV cavity volumes and EFs of 6 subjects. We proceeded to a *leave-one-out* validation approach, where the training used to compute the volumes of each subject is based on the other 5 subjects. The obtained EFs were evaluated quantitatively by comparing them with those obtained from independent manual segmentation by an expert.

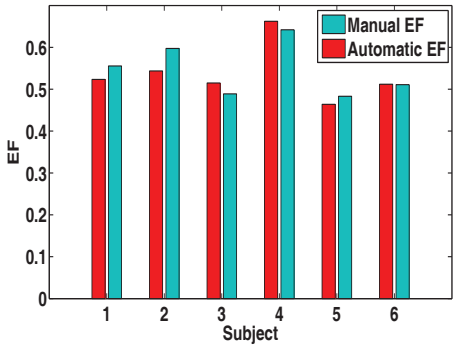


Fig. 3. Automatic and manual EFs in 6 subjects.

Let EF_A be 6 automatically estimated EFs and, EF_M containing the EFs obtained form manual segmentations. Table. 1 and Fig. 3 depict EF_A and EF_M, and confirms that the EFs computed with the proposed method are very close to those obtained from independent manual segmentations.

We evaluated the conformity between the manually and automatically computed EFs (the results are listed in Table 2). We estimated the mean and standard deviation of the norm

mean	*std*	*time*(*sec*)
0.025	0.017	0.21

Table 2. Statistical measures of the conformity between automatically and manually computed EFs and computation time (in seconds)

of the difference between EF_A and EF_M:

$$Diff_{EF} = \sum \|EF_A - EF_M\| \quad (12)$$

The very low *mean* and standard deviation (*std*) of $Diff_{EF}$ (Table 2) indicates a high conformity between manual and automatic EFs.

4. CONCLUSION

This study investigated a real-time method for computing the cardiac EF directly from image statistics via machine learning. These image statistics were based on the Bhattacharyya coefficients of similarity between image distributions, which were shown to be non-linearly related to the LV cavity areas. An ANN was used to find the relation between the image statistics and the corresponding LV cavity areas in each subject dataset. A preliminary experimental evaluation over 6 subjects demonstrated good conformity of automatically estimated EFs to those computed from manual segmentation.

5. REFERENCES

[1] HC. Han, RP. Martin, G. Lerakis, and S. Lerakis, "Prediction of the left ventricular ejection fraction improvement using echocardiography and mechanical modeling," *Journal of the American Society of Echocardiography*, vol. 18, no. 7, pp. 718–721, 2005.

[2] BL. Zaret, HW. Strauss, and PJ. Hurely, "Left ventricular ejection fraction and regional myocardial performancein man without cardiac catheterisation," *Journal of American Heart Association Circulation*, vol. 42, no. 3, pp. 649–651, 1970.

[3] J. Anthony Parker, Roger Secker-Walker, Rex Hill, Barry A. Siegel, and E. James Potchen, "A new technique for the calculation of left ventricular ejectionfraction," *Journal of Nuclear Medicine*, vol. 13, no. 8, pp. 649–651, 1972.

[4] HY Lee, Nl.C.F. Codella, M.D. Cham, J.W. Weinsaft, and W Yi, "Automatic left ventricle segmentation using iterative thresholding and an active contour model with adaptation on short-axis cardiac mri," *IEEE Trans on Biomedical Engineering*, vol. 57, no. 4, pp. 905–913, 2010.

[5] A. Pednekar, R. Muthupillai, V. V. Lenge, I.A. Kakadiaris, and S. D. Flamm, "Automatic identification of the left ventricle in cardiac cine-MR images: Dual-contrast cluster analysis and scout-geometry approaches," *Journal of Magnetic Resonance Imaging*, vol. 23, no. 5, pp. 641–651, 2006.

[6] M. Lynch, O. Ghita, and P.F. Whelan, "Automatic segmentation of the left ventricle cavity and myocardium in mri data," *Computers in Biology and Medicine*, vol. 36, no. 4, pp. 389–407, 2006.

[7] I. Ben Ayed, P. Kumaradevan, A. Islam, J. Chong, and Sh. Li, "Left ventricle segmentation via graph cut distribution matching," in *MICCAI*, 2009, vol. 5762, pp. 901–909.

[8] J. Zhu-Jacquot and R. Zabih, "Segmentation of the left ventricle in cardiac MR images using graph cuts with parametric shape priors," in *ICASSP*, 2008, pp. 521–524.

[9] M. Fradkin, C. Ciofolo, B. Mory, G. Hautvast, and M. Breeuwer, "Comprehensive segmentation of cine cardiac MR images," in *MICCAI*, 2008, vol. 5241, pp. 178–185.

[10] I. Ben Ayed, Sh. Li, and I. Ross, "Embedding overlap priors in variational left ventricle tracking," *IEEE Trans. on Medical Imaging*, vol. 28, no. 12, pp. 1902–1913, 2009.

[11] A. Andreopoulos and J. K. Tsotsos, "Efficient and generalizable statistical models of shape and appearance for analysis of cardiac MRI," *Medical Image Analysis*, vol. 12, no. 3, pp. 335–357, 2008.

[12] C. Petitjean and J-N. Dacher, "A review of segmentation methods in short axis cardiac MR images," *Medical Image Analysis*, vol. 15, no. 2, pp. 169–184, 2011.

[13] O. Michailovich, R. Yogesh, and A. Tannenbaum, "Image segmentation using active contours driven by the Bhattacharyya gradient flow," *IEEE Trans. on Image Processing*, vol. 16, no. 11, pp. 2787–2801, 2007.

[14] Laurene Fausett, Ed., *Fundamentals of neural networks: architectures, algorithms, and applications*, Prentice-Hall, Inc., Upper Saddle River, NJ, USA, 1994.